times and then immediately applied for gel electorophoresis. For dissociation experiments, incubation was for 30 min, immediately followed by addition of a 20-fold excess of unlabeled p21WT oligonucleotide to challenge the DNA-protein complex for the indicated times. The mixture was then applied for gel electorophoresis.

In vitro transcription and primer extension. In vitro transcription assays with nuclear extract were performed using the HeLaScribe nuclear extract in vitro transcription system (Promega) following the manufacturer's protocol. Briefly, reactions (25 µl) contained 20 mM HEPES (pH 7.9), 5 mM $MgSO_4$, 0.2 mM EGTA, 20% glycerol, 0.5 mM DTT, 100 mM KCl, with nucleotide ribo-triphosphates (0.4 mM each), 8 U of HeLa nuclear extract, recombinant proteins and 0.3 µg of PG13-Luc reporter plasmid, or 0.1 µg of pcDNA4A plasmid (Invitrogen). PG13-Luc[3] was gifts from Dr. B. Vogelstein (The Johns Hopkins University Medical Institutions). The reactions were allowed to proceed for 15 min at 30°C. Primer extension analysis for the RNA produced during these reactions was performed using a γ-^{32}P 5'-end-labeled oligonucleotide complementary to the luciferase coding sequence (5'-GAA GAG CCA AAA AC-3') and the pcDNA4 vector sequence (5'-TCG TTT AGT GAA CCG TCA GAT-3') as a control. The extension products were separated on a 8% polyacrylamide gel containing 0.5x TBE and 7 M urea, analyzed by autoradiography, and quantified with a BAS-2500 Imaging analyzer (Fuji Photo Film).

Luciferase reporter assay. Tet-BZLF1/HeLa cells seeded in 24-well plates were transfected with 0.05 µg of the luciferase reporter plasmid (PG13-Luc), and treated with or without Dox. The amount of transfected DNA was kept constant by adding empty vector. Luciferase activity was measured with a luciferase assay system (Promega) according to the manufacturer's instructions, using a luminometer (Berthold).

RT-PCR analysis. Isolation of total RNA from cells was performed using RNeasy spin column kits (Qiagen) and cDNAs were synthesized using SuperScript III first-strand synthesis system for RT-PCR (Invitrogen) with total RNAs as templates. The detection of *GAPDH*, *p53* and *p21$^{WAF1/CIP1}$* cDNAs was performed by PCR using as primers; 5'-GGG AAG GTG AAG GTC GGA GT-3' and 5'-AAG ACG CCA GTG GAC TCC AC-3' for GAPDH, 5'-CCC AAC AAC ACC AGC-3' and 5'-GTG GCT GGA GTG AGC-3' for p53, and 5'-GCC CAG TGG ACA GCG AGC AG-3' and 5'-ATC TGT CAT GCT GGT CTG CC-3' for *p21$^{WAF1/CIP1}$*. *GAPDH*, *p53* and *p21$^{WAF1/CIP1}$* were amplified for 17, 30 and 26 cycles, respectively. The GAPDH gene served as an internal control in the calculation of the densitometric results.

ChIP assay. Immunoprecipitation of formaldehyde-cross-linked chromatin from the Dox-induced Tet-BZLF1/HeLa cells was performed as described previously.[39] The immunoprecipitated DNAs and input DNA were analyzed by PCR using the following as primers; 5'-TTC CTC TGA AAG CTG ACT GCC-3' and 5'-CAT GTT CCT GAC GGC CAG A-3' for the *p21$^{WAF1/CIP1}$* promoter region, 5'-CAG AGT GAT AAG GGT TGT GAA GGA G-3' and 5'-AAA ACC CCA ATC CCA TCA ACC-3' for the *p53* promoter region, and 5'-CAG GAG GCC CGT GAG CGA TGG A-3' and 5'-CTG TCC CCT GCA GCA GAG CAG GTG-3' for the *p21$^{WAF1/CIP1}$*-coding region.

Quantification of viral DNA synthesis during lytic replication. Tet-BZLF1/B95-8 cells were transfected with p53 expression plasmid or GFP-expression plasmid as a control by electroporation and then added doxycycline into the culture media 1 h post-transfection for induction of the lytic replication. Dot-blot hybridization and viral genome replication was quantified as described previously.[10]

Acknowledgements

We are grateful to Drs. C. Prives, B. Vogelstein and K. Kuzushima for invaluable materials. We thank Yasuhiro Nishikawa and Kiyoko Sasaki for technical assistance. This study was supported in part by Grants-in-aid for Scientific Research on Priority Areas from the Ministry of Education, Science, Sports, Culture and Technology of Japan (no. 21022055, 20012056, 20390137 to T.T.). Y.S. was supported by the Japanese Society for a Research Fellowship of the Promotion of Science for Young Scientists.

References

1. Haffner R, Oren M. Biochemical properties and biological effects of p53. Curr Opin Genet Dev 1995; 5:84-90.
2. Ko LJ, Prives C. p53: puzzle and paradigm. Genes Dev 1996; 10:1054-72.
3. el-Deiry WS, Tokino T, Velculescu VE, Levy DB, Parsons R, Trent JM, et al. WAF1, a potential mediator of p53 tumor suppression. Cell 1993; 75:817-25.
4. Dulic V, Kaufmann WK, Wilson SJ, Tlsty TD, Lees E, Harper JW, et al. p53-dependent inhibition of cyclin-dependent kinase activities in human fibroblasts during radiation-induced G_1 arrest. Cell 1994; 76:1013-23.
5. Tsurumi T. EBV replication enzymes. Curr Top Microbiol Immunol 2001; 258:65-87.
6. Chien YC, Chen JY, Liu MY, Yang HI, Hsu MM, Chen CJ, et al. Serologic markers of Epstein-Barr virus infection and nasopharyngeal carcinoma in Taiwanese men. N Engl J Med 2001; 345:1877-82.
7. Zeng Y, Zhang LG, Wu YC, Huang YS, Huang NQ, Li JY, et al. Prospective studies on nasopharyngeal carcinoma in Epstein-Barr virus IgA/VCA antibody-positive persons in Wuzhou City, China. Int J Cancer 1985; 36:545-7.
8. Hong GK, Gulley ML, Feng WH, Delecluse HJ, Holley-Guthrie E, Kenney SC. Epstein-Barr virus lytic infection contributes to lymphoproliferative disease in a SCID mouse model. J Virol 2005; 79:13993-4003.
9. Kudoh A, Fujita M, Zhang L, Shirata N, Daikoku T, Sugaya Y, et al. Epstein-Barr virus lytic replication elicits ATM checkpoint signal transduction while providing an S-phase-like cellular environment. J Biol Chem 2005; 280:8156-63.
10. Sato Y, Kamura T, Shirata N, Murata T, Kudoh A, Iwahori S, et al. Degradation of Phosphorylated p53 by Viral Protein-ECS E3 Ligase Complex. PLoS Pathog 2009; 5:1000530.
11. Rooney CM, Rowe DT, Ragot T, Farrell PJ. The spliced BZLF1 gene of Epstein-Barr virus (EBV) transactivates an early EBV promoter and induces the virus productive cycle. J Virol 1989; 63:3109-16.
12. Urier G, Buisson M, Chambard P, Sergeant A. The Epstein-Barr virus early protein EB1 activates transcription from different responsive elements including AP-1 binding sites. EMBO J 1989; 8:1447-53.
13. Farrell PJ, Rowe DT, Rooney CM, Kouzarides T. Epstein-Barr virus BZLF1 trans-activator specifically binds to a consensus AP-1 site and is related to c-fos. EMBO J 1989; 8:127-32.
14. Takagi S, Takada K, Sairenji T. Formation of intranuclear replication compartments of Epstein-Barr virus with redistribution of BZLF1 and BMRF1 gene products. Virology 1991; 185:309-15.
15. Cayrol C, Flemington EK. The Epstein-Barr virus bZIP transcription factor Zta causes G_0/G_1 cell cycle arrest through induction of cyclin-dependent kinase inhibitors. EMBO J 1996; 15:2748-59.
16. Cayrol C, Flemington E. G_0/G_1 growth arrest mediated by a region encompassing the basic leucine zipper (bZIP) domain of the Epstein-Barr virus transactivator Zta. J Biol Chem 1996; 271:31799-802.
17. Rodriguez A, Jung EJ, Yin Q, Cayrol C, Flemington EK. Role of c-myc regulation in Zta-mediated induction of the cyclin-dependent kinase inhibitors p21 and p27 and cell growth arrest. Virology 2001; 284:159-69.
18. Chang SS, Lo YC, Chua HH, Chiu HY, Tsai SC, Chen JY, et al. Critical role of p53 in histone deacetylase inhibitor-induced Epstein-Barr virus Zta expression. J Virol 2008; 82:7745-51.

19. Sato Y, Shirata N, Kudoh A, Iwahori S, Nakayama S, Murata T, et al. Expression of Epstein-Barr virus BZLF1 immediate-early protein induces p53 degradation independent of MDM2, leading to repression of p53-mediated transcription. Virology 2009; 388:204-11.
20. el-Deiry WS, Harper JW, O'Connor PM, Velculescu VE, Canman CE, Jackman J, et al. WAF1/CIP1 is induced in p53-mediated G_1 arrest and apoptosis. Cancer Res 1994; 54:1169-74.
21. Mauser A, Holley-Guthrie E, Simpson D, Kaufmann W, Kenney S. The Epstein-Barr virus immediate-early protein BZLF1 induces both a G(2) and a mitotic block. J Virol 2002; 76:10030-7.
22. Jayaraman L, Murthy KG, Zhu C, Curran T, Xanthoudakis S, Prives C. Identification of redox/repair protein Ref-1 as a potent activator of p53. Genes Dev 1997; 11:558-70.
23. Nie Y, Li HH, Bula CM, Liu X. Stimulation of p53 DNA binding by c-Abl requires the p53 C terminus and tetramerization. Mol Cell Biol 2000; 20:741-8.
24. Chen X, Farmer G, Zhu H, Prywes R, Prives C. Cooperative DNA binding of p53 with TFIID (TBP): a possible mechanism for transcriptional activation. Genes Dev 1993; 7:1837-49.
25. Zhang Q, Gutsch D, Kenney S. Functional and physical interaction between p53 and BZLF1: implications for Epstein-Barr virus latency. Mol Cell Biol 1994; 14:1929-38.
26. Wang S, El-Deiry WS. p73 or p53 directly regulates human p53 transcription to maintain cell cycle checkpoints. Cancer Res 2006; 66:6982-9.
27. Benoit V, Hellin AC, Huygen S, Gielen J, Bours V, Merville MP. Additive effect between NFkappaB subunits and p53 protein for transcriptional activation of human p53 promoter. Oncogene 2000; 19:4787-94.
28. Deffie A, Wu H, Reinke V, Lozano G. The tumor suppressor p53 regulates its own transcription. Mol Cell Biol 1993; 13:3415-23.
29. Mauser A, Saito S, Appella E, Anderson CW, Seaman WT, Kenney S. The Epstein-Barr virus immediate-early protein BZLF1 regulates p53 function through multiple mechanisms. J Virol 2002; 76:12503-12.
30. Wu FY, Chen H, Wang SE, ApRhys CM, Liao G, Fujimuro M, et al. CCAAT/enhancer binding protein alpha interacts with ZTA and mediates ZTA-induced p21(CIP-1) accumulation and G(1) cell cycle arrest during the Epstein-Barr virus lytic cycle. J Virol 2003; 77:1481-500.
31. Rodriguez A, Armstrong M, Dwyer D, Flemington E. Genetic dissection of cell growth arrest functions mediated by the Epstein-Barr virus lytic gene product, Zta. J Virol 1999; 73:9029-38.
32. Kudoh A, Fujita M, Kiyono T, Kuzushima K, Sugaya Y, Izuta S, et al. Reactivation of lytic replication from B cells latently infected with Epstein-Barr virus occurs with high S-phase cyclin-dependent kinase activity while inhibiting cellular DNA replication. J Virol 2003; 77:851-61.
33. Casavant NC, Luo MH, Rosenke K, Winegardner T, Zurawska A, Fortunato EA. Potential role for p53 in the permissive life cycle of human cytomegalovirus. J Virol 2006; 80:8390-401.
34. Jault FM, Jault JM, Ruchti F, Fortunato EA, Clark C, Corbeil J, et al. Cytomegalovirus infection induces high levels of cyclins, phosphorylated Rb and p53, leading to cell cycle arrest. J Virol 1995; 69:6697-704.
35. Rosenke K, Samuel MA, McDowell ET, Toerne MA, Fortunato EA. An intact sequence-specific DNA-binding domain is required for human cytomegalovirus-mediated sequestration of p53 and may promote in vivo binding to the viral genome during infection. Virology 2006; 348:19-34.
36. Daikoku T, Kudoh A, Fujita M, Sugaya Y, Isomura H, Shirata N, et al. Architecture of replication compartments formed during Epstein-Barr virus lytic replication. J Virol 2005; 79:3409-18.
37. Shieh SY, Ikeda M, Taya Y, Prives C. DNA damage-induced phosphorylation of p53 alleviates inhibition by MDM2. Cell 1997; 91:325-34.
38. Hsu CH, Chang MD, Tai KY, Yang YT, Wang PS, Chen CJ, et al. HCMV IE2-mediated inhibition of HAT activity downregulates p53 function. EMBO J 2004; 23:2269-80.
39. Sato Y, Miyake K, Kaneoka H, Iijima S. Sumoylation of CCAAT/enhancer-binding protein alpha and its functional roles in hepatocyte differentiation. J Biol Chem 2006; 281:21629-39.

J_ID: Z3Q Wiley Ed. Ref. No.: 10-1394.R1 Customer A_ID: IJC25873 Date: 13-January-11 Stage: Page: 1

uicc
global cancer control

IJC
International Journal of Cancer

Bortezomib induces apoptosis in T lymphoma cells and natural killer lymphoma cells independent of Epstein-Barr virus infection

Seiko Iwata[1], Syoko Yano[1], Yoshinori Ito[2], Yoko Ushijima[1], Kensei Gotoh[2], Jun-ichi Kawada[3], Shigeyoshi Fujiwara[4], Koichi Sugimoto[5], Yasushi Isobe[5], Yukihiro Nishiyama[1] and Hiroshi Kimura[1]

[1] Department of Virology, Nagoya University Graduate School of Medicine, Nagoya, Japan
[2] Department of Pediatrics, Nagoya University Graduate School of Medicine, Nagoya, Japan
[3] Department of Infection and Immunology, Aichi Children's Health and Medical Center, Aichi, Japan
[4] Department of Infectious Diseases, National Research Institute for Child Health and Development, Tokyo, Japan
[5] Department of Hematology, Juntendo University School of Medicine, Tokyo, Japan

Epstein-Barr virus (EBV), which infects not only B cells, but also T cells and natural killer (NK) cells, is associated with multiple lymphoid malignancies. Recently, the proteasome inhibitor bortezomib was reported to induce apoptosis of EBV-transformed B cells. We evaluated the killing effect of this proteasome inhibitor on EBV-associated T lymphoma cells and NK lymphoma cells. First, we found that bortezomib treatment decreased the viability of multiple T and NK cell lines. No significant difference was observed between EBV-positive and EBV-negative cell lines. The decreased viability in response to bortezomib treatment was abrogated by a pan-caspase inhibitor. The induction of apoptosis was confirmed by flow cytometric assessment of annexin V staining. Additionally, cleavage of caspases and polyadenosine diphosphate-ribose polymerase, increased expression of phosphorylated IκB, and decreased expression of inhibitor of apoptotic proteins were detected by immunoblotting in bortezomib-treated cell lines. We found that bortezomib induced lytic infection in EBV-positive T cell lines, although the existence of EBV did not modulate the killing effect of bortezomib. Finally, we administered bortezomib to peripheral blood mononuclear cells from two patients with EBV-associated lymphoproliferative diseases. Bortezomib had a greater killing effect on EBV-infected cells. These results indicate that bortezomib killed T or NK lymphoma cells by inducing apoptosis, regardless of the presence or absence of EBV.

Key words: Epstein-Barr virus, proteasome inhibitor, apoptosis, lytic infection, NF-κB

Abbreviations: 7-AAD: 7-aminoactinomycin D; BART's: *Bam*HI-A rightward transcripts; cIAP: cellular IAP; DMSO: dimethyl sulfoxide; EBV: Epstein-Barr virus; EBER: EBV-encoded small RNA; EBNA: EBV nuclear antigen; FISH: Flow cytometric in situ hybridization; IAPs: inhibitors of apoptotic proteins; LMP: latent membrane protein; LCL: lymphoblastoid cell lines; MNCs: mononuclear cells; NK: natural killer; NF-κB: nuclear factor-κB; PBS: phosphate-buffered saline; PE: phycoerythrin; PARP: polyadenosine diphosphate-ribose polymerase; RT: reverse transcription; SDS: sodium dodecyl sulfate; XIAP: X-linked IAP; β2m: β2-microglobulin

Grant sponsor: Ministry of Education, Culture, Sports, Science and Technology, Japan; **Grant number:** 19591247; **Grant sponsor:** Ministry of Health, Labor, and Welfare of Japan [grant for research on measures for emerging and reemerging infections (Intractable Infectious Diseases in Organ Transplant Recipients, H21-Shinko-Ippan-094)]

DOI: 10.1002/ijc.25873

History: Received 17 Jun 2010; Accepted 30 Nov 2010; Online 00 Month 2011

Correspondence to: Hiroshi Kimura, Department of Virology, Nagoya University Graduate School of Medicine, 65 Tsurumai-cho, Showa-ku, Nagoya 466-8550, Japan, Tel.: +81-52-744-2451
Fax: +81-52-744-2452, E-mail: hkimura@med.nagoya-u.ac.jp

The ubiquitous Epstein-Barr virus (EBV) infects most individuals by early adulthood and typically remains latent throughout life. EBV not only infects B cells but also T cells and natural killer (NK) cells and has been associated with multiple lymphoid malignancies such as Burkitt lymphoma, diffuse large B cell lymphoma, Hodgkin lymphoma, post-transplant lymphoproliferative disorders, nasal NK/T lymphoma, hydroa vacciniforme-like lymphoma, aggressive NK cell leukemia, and chronic active EBV infection.[1–4] EBV plays an important role in the pathogenesis of many of these malignancies through its ability to establish latent infection and induce the proliferation of infected cells.[5] Some of these EBV-associated lymphoid malignancies are refractory and resistant to conventional chemotherapies. Rituximab, a humanized monoclonal antibody against CD20, targets B cell-specific surface antigens present on EBV-transformed malignant cells. Currently, Rituximab is used in the treatment and prophylaxis of B cell lymphoma and lymphoproliferative disorders.[6,7] However, a continuing need exists for effective treatments of T and NK cell lymphoid malignancies, and novel approaches of molecular target therapy are desirable.

Recently, bortezomib was reported to induce apoptosis in EBV-transformed B cells and prolong survival of mice inoculated with EBV-transformed B cells.[8] Bortezomib is an inhibitor of the 26S proteasome.[9] Proteasomes are multi-protein

ID: srinivasanv | Black Lining: [ON] | Time: 13:24 | Path: N:/Wiley/3b2/IJC#/Vol00000/100792/APPFile/JW-IJC#100792

J_ID: Z3Q Wiley Ed. Ref. No.: 10-1394.R1 Customer A_ID: IJC25873 Date: 13-January-11 Stage: Page: 2

complexes that degrade ubiquitinated proteins, including those involved in cell cycle regulation, oncogenesis, and apoptosis. Inhibition of the proteasome can result in apoptosis in malignant cells.[10,11] Bortezomib is approved for the treatment of multiple myeloma and is in clinical trials for non-Hodgkin lymphoma, prostate cancer, and lung cancer.[12,13] A key factor in the ability of bortezomib to kill myeloma cells is that it blocks the activation of nuclear factor-κB (NF-κB).[14] In normal cells, NF-κB is bound to the inhibitory protein IκB, which maintains it in an inactive form in the cytoplasm. Once activated, NF-κB can then enter the nucleus and initiate many actions in the tumor cell that help the cell to survive and proliferate. As a result of inhibiting the proteasome and thus the activation of NF-κB, bortezomib may induce apoptosis by reducing the expression of inflammatory molecules and cell adhesion molecules.[14] Additionally, a study has reported that bortezomib can lead to EBV lytic infection.[15] In EBV-infected lymphocytes, only a few viral genes are expressed to maintain latency and to avoid host immune mechanisms.[1,5] Bortezomib may alter the pattern of viral gene expression thus converting a latent infection to a lytic infection

In our study, we evaluated the killing effect of bortezomib on EBV-associated T/NK lymphoma cells. To investigate the mechanism of killing, we administered bortezomib to multiple EBV-positive and -negative T and NK cell lines. We further administered bortezomib *ex vivo* to lymphoma cells from patients with EBV-associated lymphoid malignancies.

Material and Methods

Cell lines and reagents

Raji, a latency type III cell line, is an EBV-positive B cell line derived from Burkitt lymphoma.[16] Lymphoblastoid cell lines (LCL)-1 and LCL-2, latency type III cell lines, are EBV-positive B cell lines transformed with B95-8 EBV from peripheral blood B lymphocytes. BJAB is an EBV-negative B cell line. SNT-13 and SNT-16[17] are EBV-positive T cell lines. SNK-6[17] and KAI-3[18] are EBV-positive NK cell lines. SNT-13, -16, SNK-6, and KAI-3 were derived from patients with chronic active EBV infection or nasal NK/T cell lymphomas. Jurkat[19] and KHYG-1[20] are EBV-negative T and NK cell lines, respectively. Jurkat was derived from a patient with acute T lymphoblastic leukemia. KHYG-1 was derived from a patient with aggressive NK cell leukemia.

MT-2 cell line was established from cord mononuclear cells by co-culture with adult T cell leukemia cells, and harbors human T cell-leukemia virus type I.[21] MT-2/rEBV/9-7 cell line was established by infection of MT-2 cells with the hygromycin-resistant B95-8 strain.[22] MT-2/hyg cell line, transfected with a hygromycin-resistant gene, and MT-2/rEBV/9-7 were used to verify the difference of EBV presence in the T cell lines. Similarly, NKL cell line[23] was derived from a patient with NK cell leukemia, and TL1 cell line[24] was established from NKL cells infected with Akata-transfected recombinant EBV strain containing a neomycin-resistant gene. TL1 and NKL were used to verify the difference of EBV presence in the NK cell lines.

Raji, LCL-1, LCL-2, BJAB, and Jurkat cells were grown in RPMI 1640 supplemented with 10% heat-inactivated fetal bovine serum, penicillin, and streptomycin (complete media). The medium for SNT-13, -16, KAI3, SNK-6, KHYG1, TL1, and NKL was complete media supplemented with 100 U/ml human interleukin-2. The medium for MT-2/hyg and MT-2/rEBV/9-7 was complete media supplemented with 0.2 mg/ml hygromycin. TL1 underwent periodic selection with G418.

Bortezomib, a gift from Millennium Pharmaceuticals (Cambridge, MA), was dissolved in phosphate-buffered saline (PBS). The pan-caspase inhibitor Q-VD-OPH (Calbiochem, La Jolla, CA) and the proteasome inhibitor MG132 (Biomol International, Plymouth Meeting, PA) were dissolved in dimethyl sulfoxide (DMSO).

Cell viability and apoptosis assays

Cells (2×10^5/ml) were cultured in 24-well plates and cell viability was quantified by trypan blue exclusion. The pan-caspase inhibitor Q-VD-OPH (50 μM) was added at 1 hr prior to the addition of bortezomib. These experiments were performed in duplicate and the results are shown as the mean of two wells.

Apoptosis was measured by flow cytometry using an annexin V-phycoerythrin (PE)/7-aminoactinomycin D (7-AAD) apoptosis assay kit (BD Pharmingen Biosciences, San Diego, CA) according to the manufacturer's protocol. Briefly, 2×10^5 cells were treated with various concentrations of bortezomib for 6 hr, washed with ice-cold PBS, resuspended in binding buffer, incubated with annexin V-PE and 7-AAD for 15 min, and then analyzed by flow cytometry. Viable cells were defined as those negative for annexin V-PE and 7-AAD staining, and early apoptotic cells were defined as those positive for annexin V-PE and negative for 7-AAD staining. Stained cells were analyzed using a FACSCalibur and CellQuest software (Becton Dickinson, Franklin Lakes, NJ).

Immunoblots

Whole-cell extracts were lysed directly with sodium dodecyl sulfate (SDS) sample buffer (50 mM Tris-HCl, pH 6.8, 2% SDS, 10% glycerol, 6% 2-mercaptoethanol, 0.0025% bromophenol blue). Cell lysates were separated by SDS-polyacrylamide gel electrophoresis and transferred to polyvinylidene difluoride membranes (Immobilon-P membrane; Millipore), and immunoblotted with antibodies. Antibodies were directed against caspase-3, cleaved caspase-3, caspase-9, phosphorylated IκBα, and polyadenosine diphosphate-ribose polymerase (PARP) (Cell Signaling Technology, Beverly, MA); β-actin (Sigma, St. Louis, MO); XIAP and cIAP-2 (R&D Systems, Minneapolis, MN); and p53 (BD Pharmingen Biosciences). To compare the amounts of each protein, densitometoric analysis was performed using ImageJ software ver. 1.43 (NIH, Bethesda, MD).

ID: srinivasanv | Black Lining: [ON] | Time: 13:24 | Path: N:/Wiley/3b2/IJC#/Vol00000/100792/APPFile/JW-IJC#100792

J. ID: Z3Q Wiley Ed. Ref. No.: 10-1394.R1 Customer A_ID: IJC25873 Date: 13-January-11 Stage: Page: 3

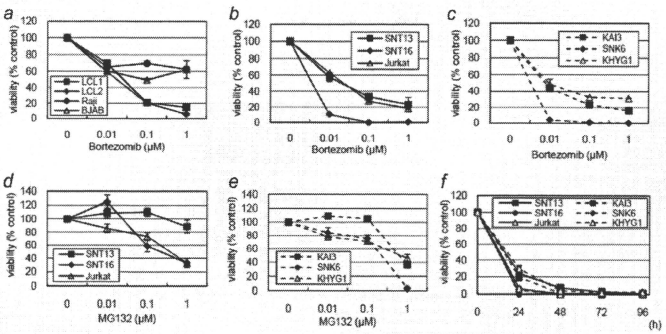

Figure 1. Bortezomib decreases the viability of B, T and NK cell lines. (*a*) B cell lines (Raji, LCL-1, LCL-2, BJAB), (*b*) T cell lines (SNT-13, SNT-16, Jurkat), and (*c*) NK cell lines (KAI-3, SNK-6, KHYG-1) were treated with bortezomib at the indicated concentrations for 24 hr. (*d*) T cell lines or (*e*) NK cell lines were treated with MG132 at various concentrations for 24 hr. (*f*) T or NK cell lines were treated with 1 μM bortezomib for 4 days and viability was determined every 24 hr. The filled markers represent EBV-positive cell lines and the open markers represent EBV-negative cell lines. Viability was calculated as the percentage of viable cells in bortezomib-treated cells *versus* PBS-treated cells. Bars indicate standard errors.

Real-time RT-PCR assay

RNA was extracted from 1×10^6 cells using the QIAmp RNeasy Mini Kit (Qiagen, Hilden, Germany). Contaminating DNA was removed by on-column deoxyribonuclease digestion using the RNase-Free DNase Set (Qiagen). Viral mRNA expression was quantified by a one-step multiplex real-time reverse transcription (RT)-PCR using a Mx3000P real-time PCR system (Stratagene, La Jolla, CA), as described previously.[25,26] The stably expressed housekeeping gene β2-microglobulin (β2m) was used as an endogenous control and reference gene for relative quantification.[27] Each experiment was conducted in triplicate and results are shown as the mean of three samples with standard errors. The Mann-Whitney *U*-test was used to compare the expression levels. p values <0.05 were deemed to be statistically significant.

Patients

Peripheral blood mononuclear cells (MNCs) were collected from five patients with EBV-associated diseases. None of these patients had received any immunosuppressive treatment such as steroid therapy or chemotherapy. Patients T-1 (7-year-old boy), T-2 (6-year-old girl), and T-3 (12-year-old boy) had hydroa vacciniforme-like lymphoma, a newly classified EBV-associated T cell lymphoma.[2] In these patients, 10∼20% of the MNCs were infected with EBV, and the EBV-infected cells were primarily γδT cells.[28] The other two patients, Patients NK-1 (14-year-old boy) and NK-2 (9-year-old boy), had chronic active EBV infection, NK cell type.[29–31] In these patients, ∼40% of MNCs were infected with EBV, and the EBV-infected cells were NK cells. MNCs from three healthy donors were used as controls. Informed consent was obtained from all participants or their guardians. Our study was approved by the institutional review board of Nagoya University Hospital.

MNCs were isolated using Ficoll-Paque (Amersham Pharmacia Biotech AB, Uppsala, Sweden) gradient centrifugation. Cells (2×10^5/ml) were cultured in RPMI 1640 supplemented with 10% heat-inactivated fetal bovine serum. For the cell viability study, each experiment was performed in duplicate, and the results are shown as the mean of two wells.

Magnetic cell sorting

The primarily infected cell fractions were separated by magnetic sorting with a TCRγ/δ$^+$ T Cell Isolation Kit or CD56 Microbeads (Miltenyi Biotec, Bergisch Gladbach, Germany). Briefly, cells were magnetically labeled with MicroBeads and separated on a column placed in the MACS separator. The flow-through was collected as a negative fraction depleted of the labeled cells. The magnetically retained cells were flushed out as the positive fraction. The respective purity and recovery rates were 98.3% and 80.0% with the TCRγ/δ$^+$ T Cell Isolation Kit, and 96.4% and 80.9% with CD56 Microbeads.

Flow cytometric in situ hybridization (FISH) assay

To verify that the sorted fraction contained EBV-infected cells, a FISH assay was used.[28] Briefly, cells were fixed with 1% acetic acid/4% paraformaldehyde, permeabilized with 0.5% Tween 20/PBS, and hybridized with a fluorescein-labeled

ID: srinivasanv | Black Lining: [ON] | Time: 13:24 | Path: N:/Wiley/3b2/IJC#/Vol00000/100792/APPFile/JW-IJC#100792

J_ID: Z3Q Wiley Ed. Ref. No.: 10-1394.R1 Customer A_ID: IJC25873 Date: 13-January-11 Stage: Page: 4

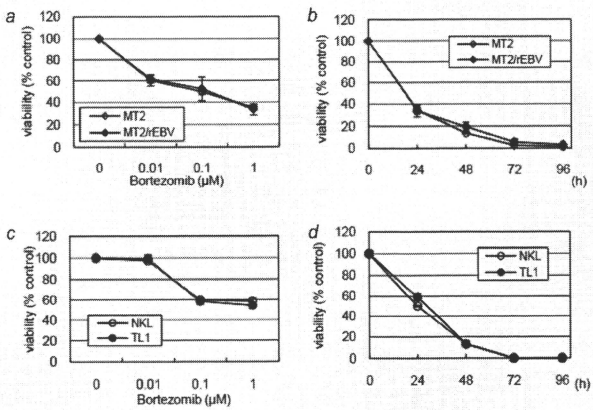

Figure 2. Bortezomib induces similar effects in EBV-positive and -negative cell lines. An EBV-positive T cell line (MT-2/rEBV) and a control cell line (MT/hyg) were treated with various concentrations of bortezomib for 24 hr (*a*) and 1 μM bortezomib for 4 days (*b*). EBV-positive NK cell line (TL1) and its parental line (NKL) were treated with various concentrations of bortezomib for 24 hr (*c*) and 1 μM bortezomib for 4 days (*d*). Bars indicate standard errors.

EBV-encoded small RNA (EBER)-specific peptide nucleic acid probe (Y5200; Dako, Glostrup, Denmark). The fluorescence intensity was enhanced using the AlexaFluor 488 Signal Amplification Kit (Molecular Probes, Eugene, OR), and stained cells were analyzed using a FACSCalibur and CellQuest software (Becton Dickinson).

Results

Bortezomib decreased the viability of B, T and NK cell lines

First, we administered bortezomib to B, T and NK cell lines for 24 hr and counted viable cells. Bortezomib decreased the viability of all four B cell lines: three EBV-positive cell lines (Raji, LCL-1, and LCL-2) and one EBV-negative cell line (BJAB; Fig. 1*a*). LCL-1 and LCL-2 were more sensitive to bortezomib than Raji or BJAB, consistent with the results of a previous study reporting that bortezomib killed both EBV-positive and -negative B cell lines, but more efficiently in LCLs.[8] Next, we administered bortezomib to T cell lines (SNT-13, SNT-16, Jurkat) and NK cell lines (KAI-3, SNK-6, KHYG-1). Bortezomib decreased the viability of all six target cell lines in a dose-dependent manner (Figs. 1*b* and 1*c*). SNT-16 and SNK-6 seemed to be more sensitive to bortezomib than other cell lines. MG132, another proteasome inhibitor, had less effect on these cell lines (Figs. 1*d* and 1*e*). We administered 1 μM bortezomib to these cell lines for 4 days and determined their viability every 24 hr. We found that bortezomib decreased the viability of these six cell lines by less than 10% at 48 hr or later (Fig. 1*f*). There were no obvious differences on the effect of bortezomib between the EBV-positive and -negative cell lines. Furthermore, to directly compare the effect of bortezomib between EBV-positive and -negative cell lines, we administered bortezomib to MT-2/hyg and MT-2/rEBV/9-9 (Figs. 2*a* and 2*b*), and NKL and TL1 (Figs. 2*c* and 2*d*). We found that bortezomib had almost equal effects on the two cell lines.

Bortezomib induces apoptosis in T and NK cell lines

The induction of apoptosis was confirmed by flow cytometry with annexin V and 7-AAD staining. Bortezomib decreased viable cells, defined as those negative for both annexin V-PE and 7-AAD staining, and increased early apoptotic cells, defined as those positive for annexin V-PE and negative for 7-AAD staining in the four cell lines (Fig. 3*a*): EBV-positive (SNT-16) and EBV-negative T cell lines (Jurkat); and EBV-positive (KAI-3) and EBV-negative NK cell lines (KHYG-1). This result showed that bortezomib induced apoptosis in both T and NK cell lines.

Next, to analyze the mechanism of bortezomib-induced apoptosis, cleavages of caspase and PARP were investigated by immunoblotting. Bortezomib induced cleavage of caspase-3, caspase-9, and PARP in all four cell lines (Fig. 3*b*). The decrease in viability caused by bortezomib was inhibited by pretreatment with Q-VD-OPH, a pan-caspase inhibitor (Fig. 3*c*).

ID: srinivasanv | Black Lining: [ON] | Time: 13:25 | Path: N:/Wiley/3b2/IJC#/Vol00000/100792/APPFile/JW-IJC#100792

J. ID: Z3Q Wiley Ed. Ref. No.: 10-1394.R1 Customer A_ID: IJC25873 Date: 13-January-11 Stage: Page: 5

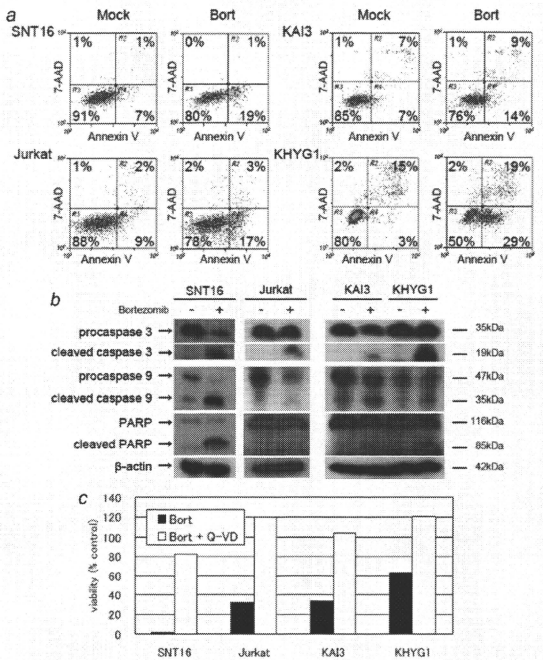

Figure 3. Bortezomib induces apoptosis in T/NK cell lines. (*a*) T cell lines (EBV-positive SNT-16 and -negative Jurkat) and NK cell lines (EBV-positive KAI-3 and -negative KHYG-1) were treated with 1 μM bortezomib for 6 hr. Viable cells were defined as those negative for annexin V-PE and 7-AAD staining, and early apoptotic cells were defined as those positive for annexin V-PE and negative for 7-AAD staining. (*b*) Bortezomib induces cleavage of caspase-3, caspase-9, and PARP. T/NK cell lines were treated with 1 μM bortezomib for 6 hr. Protein lysates were prepared and immunoblotting was performed. β-actin was used as a loading control. Each experiment was performed at least twice. (*c*) Q-VD-OPH inhibits the decrease in viability induced by bortezomib. The pan-caspase inhibitor Q-VD-OPH (50 μM) was added 1 hr prior to the addition of 1 μM bortezomib for 24 hr. Viability was calculated as the percentage of viable cells to PBS-treated cells as assessed by trypan blue exclusion.

Bortezomib blocks activation of NF-κB by inhibiting the proteasome, reducing antiapoptotic factors

In myeloma cells, bortezomib blocks the activation of NF-κB through increasing phosphorylation of IκB.[14] Thus, we confirmed the increase in phosphorylated IκB, which should have been degraded in proteasomes, in bortezomib-treated cell lines by immunoblotting (Fig. 4*a*). Furthermore, we evaluated the effect of bortezomib on two inhibitors of apoptotic proteins (IAPs). Bortezomib down-regulated cellular IAP (cIAP)-2 and X-linked IAP (XIAP) in bortezomib-treated T/NK cell lines (Fig. 4*b*). Densitometoric analysis was performed to confirm that cIAP-2 and XIAP were decreased in all bortezomib-treated cells (Fig. 4*c*). Additionally, bortezomib up-regulated p53, facilitating apoptosis, in some cell lines (Fig. 4*b*).

Bortezomib induces lytic infection of EBV in T cell lines

Next, we analyzed the expression of eight viral genes using a real-time RT-PCR assay: two lytic genes, BZLF1 and gp350/

ID: srinivasanv | Black Lining: [ON] | Time: 13:25 | Path: N:/Wiley/3b2/IJC#/Vol00000/100792/APPFile/JW-IJC#100792

J_ID: Z3Q Wiley Ed. Ref. No.: 10-1394.R1 Customer A_ID: IJC25873 Date: 13-January-11 Stage: Page: 6

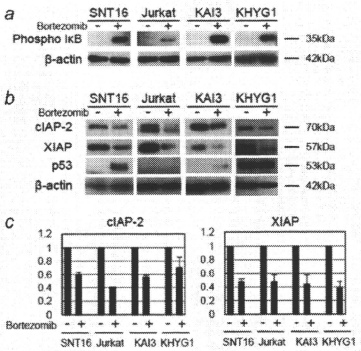

Figure 4. Bortezomib increases phosphorylated IκB and down-regulates the inhibitor of apoptotic proteins in T/NK cell lines. T cell lines (EBV-positive SNT-16 and -negative Jurkat) and NK cell lines (EBV-positive KAI-3 and -negative KHYG-1) were treated with 1 μM bortezomib for 2 hr (*a*) or 8 hr (*b*). Protein lysates were prepared and immunoblotting was performed. β-actin was used as a loading control. Each experiment was performed at least twice. (*c*) Densitometoric analysis was performed using ImageJ software. The data were calculated as the ratios of cIAP-2 (left) and XIAP (right) to β-actin, and the value of PBS-treated cells was assigned as 1. Boxes indicate the mean of two experiments and bars indicate the standard errors.

220; and six latent genes, EBV nuclear antigen (EBNA) 1, EBNA2, latent membrane protein (LMP) 1, LMP2, EBER1, and *Bam*HI-A rightward transcripts (BARTs). We found that the expression of two lytic genes, an immediate early gene (BZLF1) and a late gene (gp350/220), were increased in bortezomib-F5 treated T cell lines (SNT-13 and SNT-16 in Fig. 5). In NK cell lines, however, no such effect was observed. Regarding latent genes, expression of LMP2 was increased in T cell lines. The expressions of other latent genes (EBNA1, EBNA2, LMP1, EBER1, and BARTs) were not obviously different between bortezomib-treated cells and controls (Fig. 5).

Bortezomib decreases the viability of EBV-infected cells from patients with EBV-associated lymphoma

Finally, we investigated the *ex vivo* effect of bortezomib in MNCs from five patients with EBV-associated malignancies. We separated γδT cells and other MNCs from three patients (Patients T-1, T-2, and T-3) with hydroa vacciniforme-like lymphoma by magnetic sorting. Bortezomib (0.5 μM) was administered to each sample of cells, and the viable cells were counted for 3 days. Bortezomib had a greater killing effect on γδT cells that were primarily infected with EBV than on the other MNCs (Fig. 6*a*). Next, we separated the NK cells and other MNCs from two patients (Patients NK-1, and NK-2) with chronic active EBV infection, NK cell-type, and evaluated the effect of bortezomib. For Patient NK-1, experiments were performed twice on different visits. Bortezomib had a greater killing effect on NK cells than on the other MNCs (Fig. 6*b*). In the γδT cell or NK-cell fraction, the absolute number of control variable cells was stable or increased slightly, while the number was clearly decreased with bortezomib treatment (data not shown). Next, we collected blood samples from three healthy donors, sorted the γδT cells, NK cells, and other MNCs, and evaluated their viability with bortezomib treatment. The viability of the cells treated with bortezomib for 3 days was around 100%, indicating that bortezomib did not affect nontumor cells (Fig. 6*c*).

F6

To confirm that the sorted fractions contained EBV-infected cells, EBER-positive cells were quantified using a FISH assay. In Patient T-1 with hydroa vacciniforme-like lymphoma, 19.8% of the MNCs were EBER-positive. After magnetic sorting, 54.7% of γδT cells and 3.8% of the other MNCs were EBER-positive (Fig. 6*d*). To determine whether EBV-infected cells survive selectively, we quantified EBV-positive cells using the FISH assay after bortezomib treatment, and compared the results with PBS-treated control cells. After 3 days, the percentage of EBER-positive bortezomib-treated γδT cells decreased (4.0%), as compared to PBS-treated γδT cells (47.8%) (Fig. 6*e*). Similarly, the percentage of EBER-positive cells in bortezomib-treated NK cells decreased (0.5%), as compared to PBS-treated NK cells (34.1%) (Fig. 6*e*). These results indicate that EBV-positive cells in the control groups survived, while most EBV-positive bortezomib-treated γδT and NK cells died. Moreover, this killing effect was confirmed by flow cytometry using annexin V and 7-AAD staining in Patient NK-1 (Fig. 6*f*).

Discussion

Bortezomib, which is used in the treatment of myeloma, has also been assessed for a variety of other malignancies. In recent studies, this proteasome inhibitor was reported to induce apoptosis in NK lymphoma/leukemia cells,[32,33] and has been tested in cutaneous T cell lymphomas and aggressive T/NK cell lymphomas, including EBV-associated ones.[34,35] Although promising data have accumulated, these trials were small and must be considered preliminary. Furthermore, experience with EBV-associated cases is limited. To our knowledge, there have been no *in vitro* studies to compare the efficacy of bortezomib between EBV-positive and EBV-negative T/ NK lymphoma cells.

In our study, we treated T and NK cell lines with bortezomib to investigate this proteasome inhibitor's ability to induce apoptosis in T and NK lymphoma cells. Bortezomib markedly decreased the viability of T and NK cell lines by inducing apoptosis. Consistent with previous reports, the cleavage of caspases and PARP, increased phosphorylated IκB, and the decreased inhibitor apoptotic proteins indicated

ID: srinivasanv | Black Lining: [ON] | Time: 13:25 | Path: N:/Wiley/3b2/IJC#/Vol00000/100792/APPFile/JW-IJC#100792

J_ID: Z3Q Wiley Ed. Ref. No.: 10-1394.R1 Customer A_ID: IJC25873 Date: 13-January-11 Stage: Page: 7

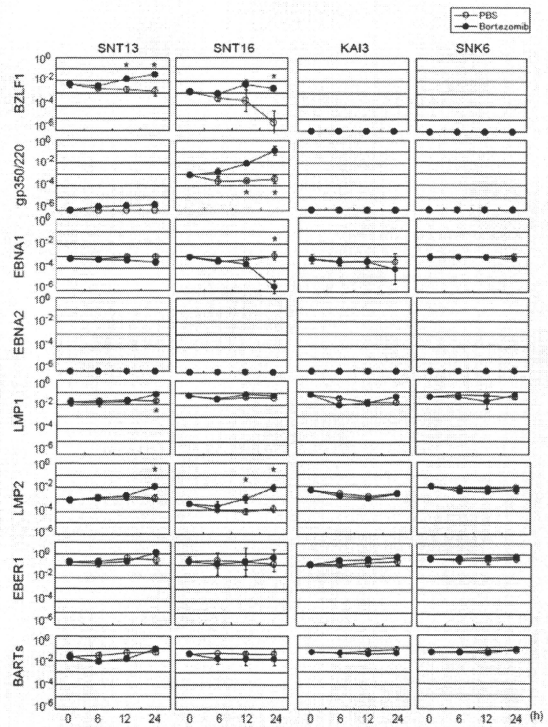

Figure 5. Bortezomib induces lytic infection of EBV in T cell lines. EBV-positive T cell lines (SNT-13 and SNT-16) and EBV-positive NK cell lines (KAI-3 and SNK-6) were treated with 1 μM bortezomib and collected at 0, 6, 12, and 24 hr to evaluate the expression of EBV-encoded genes by real-time RT-PCR. BZLF1 is an immediate early gene and gp350/220 is a late gene. EBNA1, EBNA2, LMP1, LMP2, EBER1, and BARTs are latent genes. β2-microglobulin was used as an endogenous control and reference gene for relative quantification and assigned an arbitrary value of 1 (10^0). Closed circles indicate bortezomib-treated cells, while open circles denote PBS-treated cells. Bars indicate standard errors. *$p < 0.05$ by Mann-Whitney *U*-test.

that this apoptosis was due to bortezomib inhibiting the degradation of phosphorylated IκB.[8,14,36] The inhibition of phosphorylated IκB degradation restrains the activation of NF-κB, which is associated with chemoresistance and poor survival in T and NK cell lymphomas.[37,38] We found, however, no significant difference between EBV-positive and -negative cell lines. The findings suggest that the mechanism of bortezomib in eliminating malignant cells involves the inhibition of NF-κB activation inducing apoptosis and preventing the immortalization and proliferation of cells. Other mechanisms by which bortezomib acts against malignancies, such as the stabilization of p53, disruption of the cell cycle, induction of endoplasmic reticulum stress, and increased intracellular reactive oxygen species, have been reported.[39,40]

ID: srinivasanv | Black Lining: [ON] | Time: 13:25 | Path: N:/Wiley/3b2/IJC#/Vol00000/100792/APPFile/JW-IJC#100792

J_ID: Z3Q Wiley Ed. Ref. No.: 10-1394.R1 Customer A_ID: IJC25873 Date: 13-January-11 Stage: Page: 8

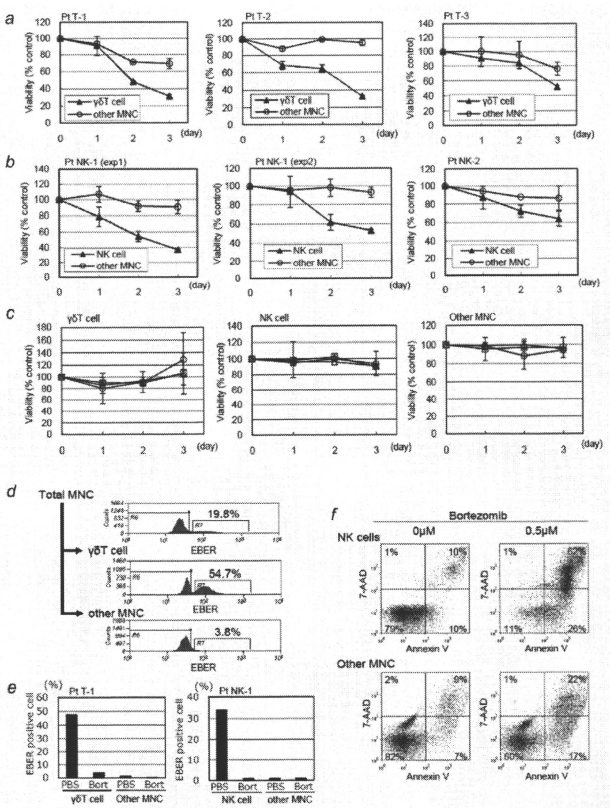

Figure 6. Bortezomib decreases the viability of EBV-infected cells from patients with EBV-associated diseases. (*a*, *b*, *c*) Bortezomib (0.5 μM) was administered to each sample of cells, and the viable cells were counted for 3 days. (*a*) γδT cells and other MNCs from three patients (Patients T-1, T-2, and T-3) with hydroa vacciniforme-like lymphoma, (*b*) NK cells and other MNCs from two patients (Patients NK-1, and NK-2) with NK cell-type chronic active EBV infection, and (*c*) γδT cell, NK cell, and non-γδT, non-NK cell (other MNC) from three healthy donors were separated by magnetic sorting. For Patient NK-1, experiments were performed twice on different visits (exp.1 and exp.2). Bars indicate standard errors. (*d*) EBER-positive cells of Patient T-1 with hydroa vacciniforme-like lymphoma were quantified using a FISH assay on unsorted MNCs (total MNCs), the γδT cell fraction (γδT cell), and the non-γδT cell fraction (other MNCs). (*e*) The EBER-positive rate of each sorted cells from Patient T-1 (left) and Patient NK-1 (right) were quantified using a FISH assay after 3 days treatment with bortezomib or PBS. (*f*) NK cells and other MNCs of Patient NK-1, with NK cell-type chronic active EBV infection were separated by magnetic sorting. Cells were treated with 0.5 μM bortezomib for 24 hr and analyzed by flow cytometry. Viable cells were defined as those negative for annexin V-PE and 7-AAD staining, and early apoptotic cells were defined as those positive for annexin V-PE and negative for 7-AAD staining.

ID: srinivasanv | Black Lining: [ON] | Time: 13:25 | Path: N:/Wiley/3b2/IJC#/Vol00000/100792/APPFile/JW-IJC#100792

J_ID: Z3Q Wiley Ed. Ref. No.: 10-1394.R1 Customer A_ID: IJC25873 Date: 13-January-11 Stage: Page: 9

The existence of EBV may have little effect on cell death induced by bortezomib. In a previous study, the killing effect of bortezomib was not different between EBV-positive and -negative Burkitt lymphoma cell lines,[8,41] although Zou *et al.*[8] reported that bortezomib had a greater effect in B cell lines with latency type III than those with Type I. The effect of bortezomib may be different in cells with different latency types due to distinct patterns of viral gene expression. The existence of EBV may have some effect on bortezomib because LMP1 is known to activate NF-κB.[42] In the study by Zou *et al.*,[8] however, transfection of LMP1 into an EBV-negative B cell line did not change the sensitivity to bortezomib. The EBV-positive T and NK cell lines used in our study are classified as latency type II[25] and express LMP1. Bortezomib seemed to have little impact on LMP1-mediated NF-κB activation because the presence of EBV did not influence its effects in our study. Comparing cell lines that are naturally EBV positive with derivative cell lines that have lost EBV is necessary to prove that EBV does not affect the outcome of bortezomib treatment. However, establishing such EBV-depleted cell lines is very difficult and, to our knowledge, there are no existing EBV-depleted T- or NK-cell lines. Alternatively, we compared EBV-negative cell lines and those that have been infected with EBV *in vitro*. We admit that this is an artificial system that may have limited relevance.

Bortezomib induced lytic infection only in T cell lines. Inhibition of the NF-κB pathway has been shown to induce the EBV lytic cycle.[43] Although the reason for the difference in lytic induction between T and NK cell lines is unclear, T cell lines seem to express lytic infection genes more often than NK cell lines, consistent with our previous report.[25] Histone deacetylase inhibitors, such as butyric acid and valproic acid, and phorbol 12-myristate 13-acetate are reported to induce an EBV lytic cycle in B cell and epithelial cell lines.[5,26] To our knowledge, however, no agent induces a lytic cycle in EBV-positive NK cell lines. We administered valproic acid, a class I histone deacetylase inhibitor, to NK-cell lymphoma cell lines. Lytic induction was not induced in the NK cell lines (data not shown).

Such lytic induction could contribute to the decreased viability of T cell lines. However, this lytic induction is not a major mechanism of bortezomib-induced cell death because no significant difference was observed in its effect between T and NK cell lines, or between EBV-positive and -negative cell lines. In SNT-16 cells, bortezomib induced a marked decrease in viability, and the recovery in viability following administration of a pan-caspase inhibitor was incomplete (Fig. 3*c*). Thus, the induction of lytic infection by bortezomib could play a partial role in this cell line. Additionally, this result suggests the potential utility of bortezomib as a novel strategy against EBV-positive T cell lymphoma. In EBV-infected T cells, a few latent genes with low antigenicity are expressed.[25] Moreover, the increased expression of lytic proteins, which are generally antigenic, can be recognized in virus-specific cytotoxic T lymphocytes, resulting in lysis of EBV-infected T cells.

Bortezomib killed EBV-infected γδT cells of hydroa vacciniforme-like lymphoma and EBV-infected NK cells of chronic active EBV infection. Taken together with the flow cytometry results, bortezomib induced apoptosis in EBV-infected immortalized cells. These results indicate that bortezomib may be an effective therapy against EBV-associated T and NK lymphoma/lymphoproliferative diseases. We administered 0.5 μM bortezomib to peripheral blood cells in an *ex vivo* study. This concentration is approximately equal to the plasma concentration after administering 1.3 mg/m^2 bortezomib in a recent Phase I and II study of multiple myeloma.[44]

Although recent studies have shown that the effect of bortezomib could be enhanced synergistically in combination with a histone deacetylase inhibitor,[45–47] further studies with appropriate *in vivo* models are essential to confirm this possibility. EBV infects only humans and no good animal models exist, although recently, humanized mouse models with reconstituted human lymphocytes and EBV infection have been reported.[48–50] Despite the complexity of this mouse model, it could be useful for evaluating new therapies, including molecular targeted therapy. The *ex vivo* administration model, coupled with magnetic sorting, is a convenient method to evaluate molecular targeted therapy against EBV-associated lymphoma.

In conclusion, bortezomib killed T/NK lymphoma cells by inducing apoptosis. No significant difference in killing was observed between EBV-positive and -negative cell lines, although bortezomib induced lytic infection in EBV-infected T cells. Following *ex vivo* administration, bortezomib had a greater killing effect on EBV-positive cells than other MNCs. These results give rationale for the use of bortezomib on T/NK lymphomas, although existence of EBV may have little effect on cell death induced by bortezomib.

Acknowledgements

We thank Norio Shimizu (Tokyo Medical and Dental University) and Ayako Demachi-Okamura (Aichi Cancer Center) for the SNK-6, SNK-10, SNT-13 and SNT-16 cell lines. KAI3 and KHYG-1 were obtained from the Japanese Collection of Research Bioresources. We also thank Millennium Pharmaceuticals Inc. for providing the bortezomib.
All authors have no conflict.

References

1. Cohen JI. Epstein-Barr virus infection. *N Engl J Med* 2000;343:481–92.
2. Quintanilla-Martinez L, Kumar H, Jaffe ES. EBV$^+$ T-cell lymphoma of childhood. In: Jaffe ES, Harris NL, Stein H, eds. WHO classification of tumours of haematopoietic and lymphoid tissues, 4th edn. Lyon: IARC Press, 2008278–28.
3. Rickinson AB, Kieff E. Epstein-Barr virus. In: Knipe DM, Howley PM, eds. Fields virology, vol. 2. Philadelphia, PA: Lippincott Williams & Wilkins, 20072655–700.
4. Williams H, Crawford DH. Epstein-Barr virus: the impact of scientific advances on clinical practice. *Blood* 2006;107:862–9.

ID: srinivasanv | Black Lining: [ON] | Time: 13:26 | Path: N:/Wiley/3b2/IJC#/Vol00000/100792/APPFile/JW-IJC#100792

J_ID: Z3Q Wiley Ed. Ref. No.: 10-1394.R1 Customer A_ID: IJC25873 Date: 13-January-11 Stage: Page: 10

5. Kieff ED, Rickinson AV. Epstein-Barr virus and its replication. In: Knipe DM, Howley PM, eds. Fields virology, vol.2. Philadelphia. PA: Lippincott Williams & Wilkins, 2007.2603–54.
6. Cartron G, Watier H, Golay J, Solal-Celigny P. From the bench to the bedside: ways to improve rituximab efficacy. *Blood* 2004;104:2635–42.
7. Heslop HE. How I treat EBV lymphoproliferation. *Blood* 2009;114: 4002–8.
8. Zou P, Kawada J, Pesnicak L, Cohen JI. Bortezomib induces apoptosis of Epstein-Barr virus (EBV)-transformed B cells and prolongs survival of mice inoculated with EBV-transformed B cells. *J Virol* 2007;81: 10029–36.
9. Adams J. Proteasome inhibition: a novel approach to cancer therapy. *Trends Mol Med* 2002;8:S49–54.
10. Orlowski RZ, Eswara JR, Lafond-Walker A, Grever MR, Orlowski M, Dang CV. Tumor growth inhibition induced in a murine model of human Burkitt's lymphoma by a proteasome inhibitor. *Cancer Res* 1998;58: 4342–8.
11. Zhang XM, Lin H, Chen C, Chen BD. Inhibition of ubiquitin-proteasome pathway activates a caspase-3-like protease and induces Bcl-2 cleavage in human M-07e leukaemic cells. *Biochem J* 1999;340(Pt 1):127–33.
12. Jackson G, Einsele H, Moreau P, Miguel JS. Bortezomib, a novel proteasome inhibitor, in the treatment of hematologic malignancies. *Cancer Treat Rev* 2005;31: 591–602.
13. Richardson PG, Mitsiades C, Hideshima T, Anderson KC. Bortezomib: proteasome inhibition as an effective anticancer therapy. *Annu Rev Med* 2006;57:33–47.
14. Paramore A, Frantz S. Bortezomib. *Nat Rev Drug Discov* 2003;2:611–2.
15. Fu DX, Tanhehco YC, Chen J, Foss CA, Fox JJ, Lemas V, Chong JM, Ambinder RF, Pomper MG. Virus-associated tumor imaging by induction of viral gene expression. *Clin Cancer Res* 2007;13:1453–8.
16. Pulvertaft JV. A study of malignant tumours in Nigeria by short-term tissue culture. *J Clin Pathol* 1965;18:261–73.
17. Zhang Y, Nagata H, Ikeuchi T, Mukai H, Oyoshi MK, Demachi A, Morio T, Wakiguchi H, Kimura N, Shimizu N, Yamamoto K. Common cytological and cytogenetic features of Epstein-Barr virus (EBV)-positive natural killer (NK) cells and cell lines derived from patients with nasal T/NK-cell lymphomas, chronic active EBV infection and hydroa vacciniforme-like eruptions. *Br J Haematol* 2003;121:805–14.
18. Tsuge I, Morishima T, Morita M, Kimura H, Kuzushima K, Matsuoka H. Characterization of Epstein-Barr virus (EBV)-infected natural killer (NK) cell proliferation in patients with severe mosquito allergy; establishment of an IL-2-dependent NK-like cell line. *Clin Exp Immunol* 1999;115:385–92.
19. Kaplan J, Tilton J, Peterson WD, Jr. Identification of T cell lymphoma tumor antigens on human T cell lines. *Am J Hematol* 1976;1:219–23.
20. Yagita M, Huang CL, Umehara H, Matsuo Y, Tabata R, Miyake M, Konaka Y, Takatsuki K. A novel natural killer cell line (KHYG-1) from a patient with aggressive natural killer cell leukemia carrying a p53 point mutation. *Leukemia* 2000;14:922–30.
21. Miyoshi I, Kubonishi I, Yoshimoto S, Akagi T, Ohtsuki Y, Shiraishi Y, Nagata K, Hinuma Y. Type C virus particles in a cord T-cell line derived by co-cultivating normal human cord leukocytes and human leukaemic T cells. *Nature* 1981;294:770–1.
22. Fujiwara S, Ono Y. Isolation of Epstein-Barr virus-infected clones of the human T-cell line MT-2: use of recombinant viruses with a positive selection marker. *J Virol* 1995;69:3900–3.
23. Robertson MJ, Cochran KJ, Cameron C, Le JM, Tantravahi R, Ritz J. Characterization of a cell line, NKL, derived from an aggressive human natural killer cell leukemia. *Exp Hematol* 1996;24:406–15.
24. Isobe Y, Sugimoto K, Matsuura I, Takada K, Oshimi K. Epstein-Barr virus renders the infected natural killer cell line, NKL resistant to doxorubicin-induced apoptosis. *Br J Cancer* 2008;99:1816–22.
25. Iwata S, Wada K, Tobita S, Gotoh K, Ito Y, Demachi-Okamura A, Shimizu N, Nishiyama Y, Kimura H. Quantitative analysis of Epstein-Barr virus (EBV)-related gene expression in patients with chronic active EBV infection. *J Gen Virol* 2010;91:42–50.
26. Kubota N, Wada K, Ito Y, Shimoyama Y, Nakamura S, Nishiyama Y, Kimura H. One-step multiplex real-time PCR assay to analyse the latency patterns of Epstein-Barr virus infection. *J Virol Methods* 2008;147: 26–36.
27. Patel K, Whelan PJ, Prescott S, Brownhill SC, Johnston CF, Selby PJ, Burchill SA. The use of real-time reverse transcription-PCR for prostate-specific antigen mRNA to discriminate between blood samples from healthy volunteers and from patients with metastatic prostate cancer. *Clin Cancer Res* 2004;10:7511–9.
28. Kimura H, Miyake K, Yamauchi Y, Nishiyama K, Iwata S, Iwatsuki K, Gotoh K, Kojima S, Ito Y, Nishiyama Y. Identification of Epstein-Barr virus (EBV)-infected lymphocyte subtypes by flow cytometric in situ hybridization in EBV-associated lymphoproliferative diseases. *J Infect Dis* 2009;200:1078–87.
29. Kimura H, Hoshino Y, Hara S, Sugaya N, Kawada J, Shibata Y, Kojima S, Nagasaka T, Kuzushima K, Morishima T. Differences between T cell-type and natural killer cell-type chronic active Epstein-Barr virus infection. *J Infect Dis* 2005;191:531–9.
30. Kimura H, Hoshino Y, Kanegane H, Tsuge I, Okamura T, Kawa K, Morishima T. Clinical and virologic characteristics of chronic active Epstein-Barr virus infection. *Blood* 2001;98:280–6.
31. Kimura H, Morishima T, Kanegane H, Ohga S, Hoshino Y, Maeda A, Imai S, Okano M, Morio T, Yokota S, Tsuchiya S, Yachie A, et al. Prognostic factors for chronic active Epstein-Barr virus infection. *J Infect Dis* 2003;187:527–33.
32. Shen L, Au WY, Guo T, Wong KY, Wong ML, Tsuchiyama J, Yuen PW, Kwong YL, Liang RH, Srivastava G. Proteasome inhibitor bortezomib-induced apoptosis in natural killer (NK)-cell leukemia and lymphoma: an in vitro and in vivo preclinical evaluation. *Blood* 2007;110: 469–70.
33. Shen L, Au WY, Wong KY, Shimizu N, Tsuchiyama J, Kwong YL, Liang RH, Srivastava G. Cell death by bortezomib-induced mitotic catastrophe in natural killer lymphoma cells. *Mol Cancer Ther* 2008;7:3807–15.
34. Lee J, Suh C, Kang HJ, Ryoo BY, Huh J, Ko YH, Eom HS, Kim K, Park K, Kim WS. Phase I study of proteasome inhibitor bortezomib plus CHOP in patients with advanced, aggressive T-cell or NK/T-cell lymphoma. *Ann Oncol* 2008;19:2079–83.
35. Zinzani PL, Musuraca G, Tani M, Stefoni V, Marchi E, Fina M, Pellegrini C, Alinari L, Derenzini E, de Vivo A, Sabattini E, Pileri S, et al. Phase II trial of proteasome inhibitor bortezomib in patients with relapsed or refractory cutaneous T-cell lymphoma. *J Clin Oncol* 2007;25:4293–7.
36. Hideshima T, Richardson P, Chauhan D, Palombella VJ, Elliott PJ, Adams J, Anderson KC. The proteasome inhibitor PS-341 inhibits growth, induces apoptosis, and overcomes drug resistance in human multiple myeloma cells. *Cancer Res* 2001; 61:3071–6.
37. Kim K, Ryu K, Ko Y, Park C. Effects of nuclear factor-kappaB inhibitors and its implication on natural killer T-cell lymphoma cells. *Br J Haematol* 2005;131: 59–66.
38. Liu X, Wang B, Ma X, Guo Y. NF-kappaB activation through the alternative pathway correlates with chemoresistance and poor survival in extranodal NK/T-cell lymphoma, nasal type. *Jpn J Clin Oncol* 2009;39:418–24.
39. Chen S, Blank JL, Peters T, Liu XJ, Rappoli DM, Pickard MD, Menon S, Yu J, Driscoll DL, Lingaraj T, Burkhardt AL, Chen W,

ID: srinivasanv | Black Lining: [ON] | Time: 13:26 | Path: N:/Wiley/3b2/IJC#/Vol00000/100792/APPFile/JW-IJC#100792

J_ID: Z3Q Wiley Ed. Ref. No.: 10-1394.R1 Customer A_ID: IJC25873 Date: 13-January-11 Stage: Page: 11

et al. Genome-wide siRNA screen for modulators of cell death induced by proteasome inhibitor bortezomib. *Cancer Res* 2010;70:4318–26.
40. Nencioni A, Grunebach F, Patrone F, Ballestrero A, Brossart P. Proteasome inhibitors: antitumor effects and beyond. *Leukemia* 2007;21:30–6.
41. Cordova C, Munker R. The presence or absence of latent Epstein-Barr virus does not alter the sensitivity of Burkitt's lymphoma cell lines to proteasome inhibitors. *Acta Haematol* 2008;119:241–3.
42. Shair KH, Bendt KM, Edwards RH, Bedford EC, Nielsen JN, Raab-Traub N. EBV latent membrane protein 1 activates Akt, NFkappaB, and Stat3 in B cell lymphomas. *PLoS Pathog* 2007;3:e166.
43. Brown HJ, Song MJ, Deng H, Wu TT, Cheng G, Sun R. NF-kappaB inhibits gammaherpesvirus lytic replication. *J Virol* 2003;77:8532–40.
44. Ogawa Y, Tobinai K, Ogura M, Ando K, Tsuchiya T, Kobayashi Y, Watanabe T, Maruyama D, Morishima Y, Kagami Y, Taji H, Minami H, et al. Phase I and II pharmacokinetic and pharmacodynamic study of the proteasome inhibitor bortezomib in Japanese patients with relapsed or refractory multiple myeloma. *Cancer Sci* 2008;99:140–4.
45. Heider U, Rademacher J, Lamottke B, Mieth M, Moebs M, von Metzler I, Assaf C, Sezer O. Synergistic interaction of the histone deacetylase inhibitor SAHA with the proteasome inhibitor bortezomib in cutaneous T cell lymphoma. *Eur J Haematol* 2009;82:440–9.
46. Kawada J, Zou P, Mazitschek R, Bradner JE, Cohen JI. Tubacin kills Epstein-Barr virus (EBV)-Burkitt lymphoma cells by inducing reactive oxygen species and EBV lymphoblastoid cells by inducing apoptosis. *J Biol Chem* 2009;284:17102–9.
47. Stamatopoulos B, Meuleman N, De Bruyn C, Mineur P, Martiat P, Bron D, Lagneaux L. Antileukemic activity of valproic acid in chronic lymphocytic leukemia B cells defined by microarray analysis. *Leukemia* 2009;23:2281–9.
48. Yajima M, Imadome K, Nakagawa A, Watanabe S, Terashima K, Nakamura H, Ito M, Shimizu N, Honda M, Yamamoto N, Fujiwara S. A new humanized mouse model of Epstein-Barr virus infection that reproduces persistent infection, lymphoproliferative disorder, and cell-mediated and humoral immune responses. *J Infect Dis* 2008;198:673–82.
49. Hong GK, Gulley ML, Feng WH, Delecluse HJ, Holley-Guthrie E, Kenney SC. Epstein-Barr virus lytic infection contributes to lymphoproliferative disease in a SCID mouse model. *J Virol* 2005;79:13993–4003.
50. Strowig T, Gurer C, Ploss A, Liu YF, Arrey F, Sashihara J, Koo G, Rice CM, Young JW, Chadburn A, Cohen JI, Munz C. Priming of protective T cell responses against virus-induced tumors in mice with human immune system components. *J Exp Med* 2009;206:1423–34.

ID: srinivasanv | Black Lining: [ON] | Time: 13:26 | Path: N:/Wiley/3b2/IJC#/Vol00000/100792/APPFile/JW-IJC#100792

Journal of General Virology (2010), **91**, 42–50 DOI 10.1099/vir.0.013482-0

Quantitative analysis of Epstein–Barr virus (EBV)-related gene expression in patients with chronic active EBV infection

Seiko Iwata,[1] Kaoru Wada,[1] Satomi Tobita,[1] Kensei Gotoh,[2] Yoshinori Ito,[2] Ayako Demachi-Okamura,[3] Norio Shimizu,[4] Yukihiro Nishiyama[1] and Hiroshi Kimura[1]

Correspondence
Hiroshi Kimura
hkimura@med.nagoya-u.ac.jp

[1]Department of Virology, Nagoya University Graduate School of Medicine, Nagoya, Japan

[2]Department of Pediatrics, Nagoya University Graduate School of Medicine, Nagoya, Japan

[3]Division of Immunology, Aichi Cancer Center Research Institute, Nagoya, Japan

[4]Department of Virology, Division of Medical Science, Medical Research Institute, Graduate School of Medicine, Tokyo Medical and Dental University, Tokyo, Japan

Chronic active Epstein–Barr virus (CAEBV) infection is a systemic Epstein–Barr virus (EBV)-positive lymphoproliferative disorder characterized by persistent or recurrent infectious mononucleosis-like symptoms in patients with no known immunodeficiency. The detailed pathogenesis of the disease is unknown and no standard treatment regimen has been developed. EBV gene expression was analysed in peripheral blood samples collected from 24 patients with CAEBV infection. The expression levels of six latent and two lytic EBV genes were quantified by real-time RT-PCR. EBV-encoded small RNA 1 and *Bam*HI-A rightward transcripts were abundantly detected in all patients, and latent membrane protein (LMP) 2 was observed in most patients. EBV nuclear antigen (EBNA) 1 and LMP1 were detected less frequently and were expressed at lower levels. EBNA2 and the two lytic genes were not detected in any of the patients. The pattern of latent gene expression was determined to be latency type II. EBNA1 was detected more frequently and at higher levels in the clinically active patients. Quantifying EBV gene expression is useful in clarifying the pathogenesis of CAEBV infection and may provide information regarding a patient's disease prognosis, as well as possible therapeutic interventions.

Received 22 May 2009
Accepted 25 September 2009

INTRODUCTION

Epstein–Barr virus (EBV) is the causative agent of infectious mononucleosis and is associated with several malignancies, including Burkitt's lymphoma, Hodgkin's lymphoma, nasopharyngeal carcinoma and post-transplant lymphoproliferative disorders (Cohen, 2000; Rickinson & Kieff, 2007; Williams & Crawford, 2006). Chronic active EBV (CAEBV) infection is a systemic EBV-positive lymphoproliferative disorder characterized by persistent or recurrent infectious mononucleosis-like symptoms in patients with no known immunodeficiency (Kimura, 2006; Okano *et al.*, 2005; Straus, 1988; Tosato *et al.*, 1985). The clonal expansion of EBV-infected T cells or natural killer (NK) cells plays a pathogenic role in patients with CAEBV, particularly among those in east Asia or central America (Kanegane *et al.*, 2002; Kimura, 2006; Quintanilla-Martinez *et al.*, 2000). These patients can be classified into two groups based on the predominantly infected cell type, T cells or NK cells (Kimura *et al.*, 2001, 2003). Nonetheless, the detailed pathogenesis of CAEBV remains elusive and no standard treatment regimen has been developed. Recently, haematopoietic stem cell transplantation (HSCT) was introduced as a curative therapy for CAEBV (Fujii *et al.*, 2000; Okamura *et al.*, 2000; Taketani *et al.*, 2002); however, transplant-related complications are common in such patients (Gotoh *et al.*, 2008; Kimura *et al.*, 2001, 2003). Alternatively, the EBV-related antigens expressed by infected cells are possible targets for treatment with EBV-specific cytotoxic T lymphocytes (CTLs) (Heslop *et al.*, 1996; Rooney *et al.*, 1998).

Viral gene expression in EBV-associated diseases is classified into one of three latency patterns (Cohen, 2000; Kieff & Rickinson, 2007). Latency type I, which is found in Burkitt's lymphoma, is characterized by EBV nuclear antigen (EBNA) 1, EBV-encoded small RNAs (EBERs) and *Bam*HI-A rightward transcripts (BARTs) expression (Tao *et al.*, 1998). In latency type II, which is characteristic

A supplementary table of primer sequences is available with the online version of this paper.

of Hodgkin's lymphoma and nasopharyngeal carcinoma, EBNA1, latent membrane protein (LMP) 1, LMP2, EBERs and BARTs are expressed (Brooks *et al.*, 1992; Deacon *et al.*, 1993). In latency type III, which is associated with post-transplant lymphoproliferative disorders, all of the above latent genes (EBNA1, EBNA2, EBNA3A, 3B, 3C, EBNA-LP, LMP1, LMP2, EBERs and BARTs) are expressed (Young *et al.*, 1989).

We recently reported that EBV gene expression could be quantitatively assessed by multiplex real-time RT-PCR (Kubota *et al.*, 2008). This method not only helps quantify EBV gene expression but also can be used to clarify the pathogenesis of EBV-associated diseases and to provide information about their prognosis and possible therapeutic interventions. Thus, in this study, we quantified the expression of six latent (EBNA1, EBNA2, LMP1, LMP2, EBER1 and BARTs) and two lytic [BZLF1 and glycoprotein (gp) 350/220] EBV genes in the peripheral blood of patients with CAEBV.

RESULTS

First, we quantified the expression of several EBV genes in B, T and NK cell lines by real-time RT-PCR (Fig. 1a). In the EBV-positive B cell lines (Raji, LCL-1 and LCL-2), all six latent genes (EBNA1, EBNA2, LMP1, LMP2, EBER1 and BARTs) were detected, and the gene expression pattern was consistent with latency type III. Both lytic genes were detected in LCL-1 and -2 cells. However, none of the target genes was detected in BJAB, an EBV-negative cell line. EBNA1, LMP1, LMP2, EBER1 and BARTs, but not EBNA2, were detected in both the T (SNT-8, -13, -15 and -16) and NK cell lines (SNK-1, -6, -10 and KAI-3). The pattern of expression in the T and NK cell lines was latency type II.

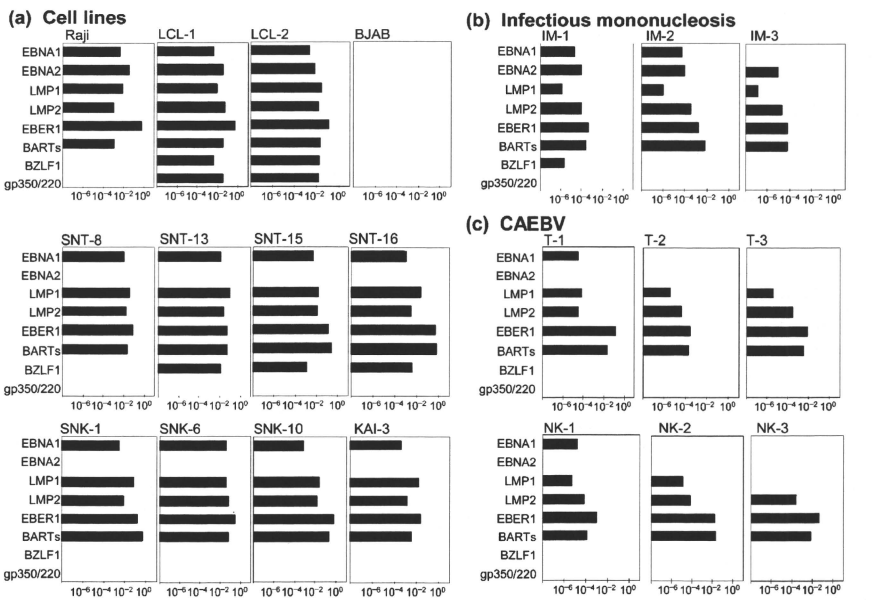

Fig. 1. Analysis of EBV gene expression by real-time RT-PCR. β2-Microglobin (β2 m) was used as an endogenous control and reference gene for relative quantification and was assigned an arbitrary value of 1 (10^0). (a) The quantity of each EBV gene in B, T and NK cells. Raji, LCL-1 and LCL-2 are EBV-positive B cell lines. BJAB is an EBV-negative B cell line. SNT-8, -13, -15 and -16 are EBV-positive T cell lines. SNK-1, -6, -10 and KAI-3 are EBV-positive NK cell lines. (b) Quantitative expression of the EBV genes in patients with infectious mononucleosis. (c) Representative results showing the relative expression of EBV genes in patients with a CAEBV infection. T-1, -2 and -3 are T-cell-type cases (patients 6, 9 and 11 in Table 1), while NK-1, -2 and -3 are NK-cell-type cases (patients 14, 15 and 19 in Table 1).

BZLF1 was detected in three of four T-cell lines, while gp350/220 was not detected in any of the cell lines, indicating an abortive lytic cycle. These results are consistent with those from previous reports (Leenman *et al.*, 2004; Tao *et al.*, 1998; Tsuge *et al.*, 1999; Zhang *et al.*, 2003), indicating the reliability of our system. We evaluated the sensitivity for each latent EBV gene using a cell mixture containing 1×10^6 EBV-negative BJAB cells and 10-fold serial dilutions of LCL-1 with latency III. The detection limits for EBNA1, EBNA2, LMP1, LMP2, EBER1 and BARTs were 0.1, 0.1, 0.01, 0.01, 0.001 and 0.01 % of LCL-1 cells, respectively. To evaluate the sensitivity for lytic genes, cell mixtures containing BJAB and Akata cells with a lytic infection, induced by human immunoglobulin G, were used. The detection limits for BZLF1 and gp350/220 were 0.1 % of Akata cells.

Next, we analysed blood from three patients with acute-phase infectious mononucleosis (Fig. 1b). EBNA2, LMP1, LMP2, EBER1 and BARTs were detected in the PBMCs of the patients, whereas EBNA1 was detected in two patients. The gene expression pattern in each case was latency type III. BZLF1 was detected in one patient, whereas gp350/220 was not detected in any patient. Furthermore, we analysed the PBMCs of 23 healthy carriers. Four healthy carriers were positive for EBV DNA. Real-time RT-PCR detected EBER1 and BARTs in the PBMCs of one carrier, while EBER1 alone was detected in a single additional carrier.

We next quantified the expression level of each gene in 24 patients with CAEBV. PBMCs collected at the time of diagnosis or referral were used in the analysis. The expression profiles of each patient are shown in Table 1, while the positive rates for each EBV gene are summarized in Table 2. EBER1 and BARTs were detected in each patient, while LMP2 was detected in most patients. EBNA1 and LMP1 were detected less frequently compared with EBER1 and BARTs ($P<0.0001$ and $P=0.004$, respectively). EBNA2 and the lytic genes BZLF1 and gp350/220 were undetected in all of the patients. Representative

Table 1. Characteristics and EBV gene expression profiles of 24 patients with chronic active EBV infection

ND, Not done. EBNA2, BZLF1 and gp350/220 were not expressed in any samples. EBER1 and BARTs were expressed in all samples.

Patient	Age (years)	Gender	Cell type infected	Viral load*				Disease type†	HSCT	Outcome	Viral load‡	EBV gene expression		
				PBMC	$CD3^+$	$CD19^+$	$CD56^+$					EBNA1	LMP1	LMP2
1	6	M	T	85925	**157196**	32828	62047	I	−	Alive	241000	−	+	+
2	5	M	T	74915	**119024**	12292	**77651**	I	−	Alive	392203	+	−	+
3	25	M	T	10749	**12106**	2742	5739	I	−	Alive	297	−	−	−
4	10	M	T	18308	**23422**	12665	**27106**	I	−	Alive	19363	−	+	+
5	6	M	T	14162	**22559**	1583	1073	A	+	Alive	14162	−	−	+
6	4	F	T	15776	**17312**	5243	4321	A	+	Alive	15776	+	+	+
7	11	M	T	60097	**143852**	23212	6352	A	+	Alive	60097	−	−	+
8	18	F	T/B	93458	**118026**	**174042**	**267078**	A	+	Alive	392734	+	+	+
9	14	F	T	30633	**32730**	8345	4760	I	+	Alive	30633	−	+	+
10	24	F	T	8589	**43469**	2388	**12555**	A	−	Dead	37148	+	−	+
11	23	F	T	5684	**7990**	4200	250	I	+	Dead	2764	−	+	+
12	13	M	T	3176	**3579**	948	839	I	+	Dead	10681	+	+	+
13	16	F	T	52978	**55431**	37536	**84110**	I	+	Dead	52978	−	+	+
14	11	M	NK	370000	31600	100000	**1800000**	I	−	Alive	339589	+	+	+
15	9	M	NK	77884	7428	17083	**89352**	I	−	Alive	89930	−	+	+
16	4	M	NK	74550	11288	18423	**86361**	A	+	Alive	74550	+	+	+
17	5	F	NK	11200	330	3300	**23400**	A	+	Alive	1108	+	+	+
18	3	M	NK	131957	1591	16450	**917500**	I	+	Alive	131957	−	+	+
19	9	M	NK	263429	92057	206565	**425956**	I	+	Alive	263429	−	−	+
20§	26	F	NK	18889	ND	ND	ND	I	+	Alive	18889	−	+	−
21	14	F	NK	1559	53	105	**4302**	A	−	Dead	1051	−	−	−
22	14	F	NK	20126	3288	1866	**35252**	I	+	Dead	44750	+	+	+
23§	16	M	NK	69121	ND	ND	ND	I	+	Dead	69121	+	+	+
24§	14	F	NK	1041	ND	ND	ND	I	+	Dead	1041	−	−	−

*Bold type indicates that EBV DNA was concentrated by fractionation; copies $(\mu g\ DNA)^{-1}$.

†Patients with severe symptoms were defined as having a clinically active disease (A); patients with no symptoms or with only skin symptoms were defined as having an inactive disease (I).

‡Indicates the EBV DNA in the PBMCs used for real-time RT-PCR analysis; copies $(\mu g\ DNA)^{-1}$.

§Infection was confirmed by *in situ* hybridization with EBER using fractionated cells.

Table 2. Detection of eight EBV-related genes in 24 patients with a CAEBV infection

Gene	No. positive patients (%)	*P*-value*
EBNA1	10 (42)	<0.001
EBNA2	0 (0)	<0.001
LMP1	16 (67)	0.004
LMP2	20 (83)	0.11
EBER1	24 (100)	–
BARTs	24 (100)	–
BZLF1	0 (0)	<0.001
gp350/220	0 (0)	<0.001

*Comparison with EBER1 and BARTs. All *P*-values were obtained using Fisher's exact test.

quantitative results for each EBV gene are shown in Fig. 1(c).

The negative results obtained for EBNA1 and LMP1 raise the possibility that the test was not sensitive enough to detect low levels of expression. Therefore, we examined the correlation between the relative expression level for each gene and the EBV DNA load in the PBMCs (Fig. 2). For all of the EBV genes examined, the expression level correlated with the EBV DNA load. However, the samples with a low EBV DNA load were not always negative for EBNA1; similar findings were seen for LMP1.

To confirm the EBV gene expression profiles in various cell populations, we separated $CD3^+$, $CD19^+$ and $CD56^+$ cells from the PBMCs by immunomagnetic sorting and quantified the gene expression in each population by real-time RT-PCR using selected patients and healthy carriers. In one patient with T-cell-type CAEBV (patient 2 in Table 1; $CD3^+$ $CD56^+$ T cells harboured EBV), type II latent genes, such as EBNA1, LMP2, EBER1 and BARTs, were detected in both the $CD3^+$ and $CD56^+$ cell populations (Fig. 3a). In a patient with NK-cell-type CAEBV (patient 14 in Table 1), type II latent genes were detected primarily in the $CD56^+$ population (Fig. 3b). On the other hand, in a healthy carrier, EBER1 and BARTs were detected in the $CD19^+$ population (presumed to be the B-cell fraction; Fig. 3c). Importantly, the gene expression profiles in the mainly infected cells largely corresponded to those in the unsorted PBMCs in all three cases, suggesting that our PBMC data could be applied to the cells in the mainly infected population.

We next estimated the mean expression level for each EBV gene in 24 patients with CAEBV (Fig. 4a). EBER1 had the highest relative expression level, followed by BARTs, LMP2 and EBNA1, whereas LMP1 had the lowest. Next, we compared the expression level for each EBV gene between the T- and NK-cell types of CAEBV (Fig. 4b). No significant difference was found, although LMP2 expression tended to be higher in the T-cell type (P=0.09). We also compared the expression levels between the clinically active patients, who presented with severe symptoms at the time of sample collection, and clinically inactive patients (Fig. 4c). EBNA1 expression was 8.3 times higher in the active patients than in the inactive patients (P=0.02). Additionally, the rate of EBNA1-positive patients in the active group was significantly higher (75 versus 25%; P=0.03). On the other hand, there was no difference in EBV DNA load in the peripheral blood between the active and inactive groups [$10^{4.4}$ versus $10^{4.5}$ copies (μg DNA)$^{-1}$; P=0.85]. We also investigated whether EBV gene expression at the time of diagnosis or referral to our hospital was associated with the subsequent disease outcome. We divided the patients into three groups: survivors without HSCT, survivors with HSCT and non-survivors. No significant difference was observed in the gene expression profiles of the three groups (Fig. 4d).

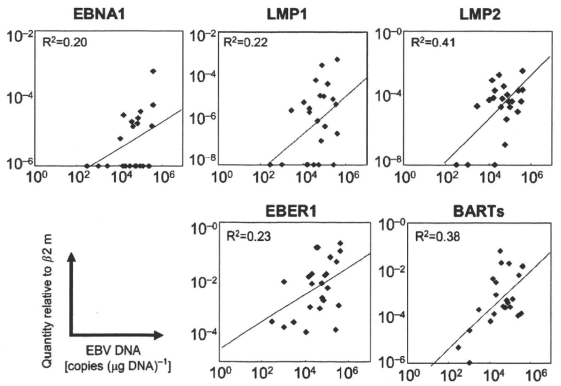

Fig. 2. Relationship between the quantity of each EBV gene and the EBV DNA load in PBMCs from patients with CAEBV. The correlation in all of these was statistically significant.

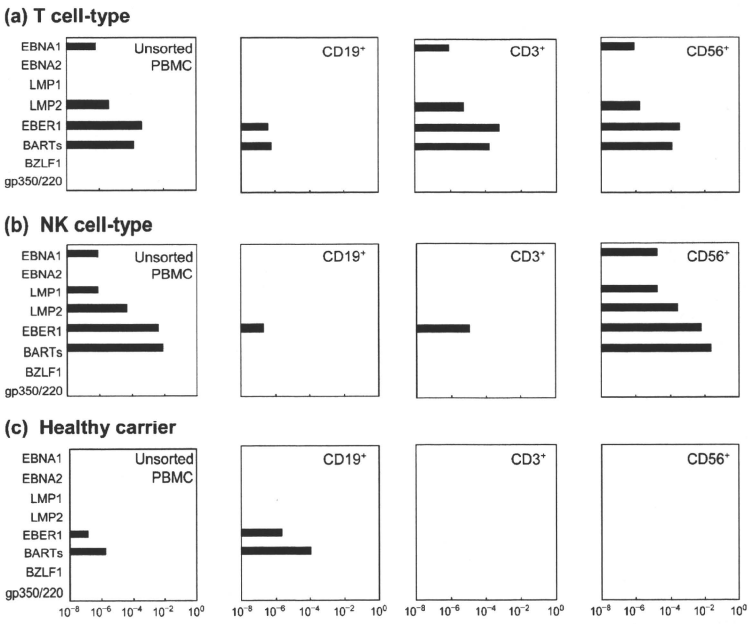

Fig. 3. EBV gene expression in sorted cell populations. $CD19^+$, $CD3^+$ and $CD56^+$ cells were separated by immunomagnetic sorting and analysed by real-time RT-PCR; unsorted PBMCs were analysed. (a) A T-cell-type CAEBV patient (patient 2 in Table 1; $CD3^+$ $CD56^+$ T cells were the main type of infected cells). (b) An NK-cell-type CAEBV patient (patient 14 in Table 1). (c) A healthy carrier whose PBMCs were positive for EBV DNA.

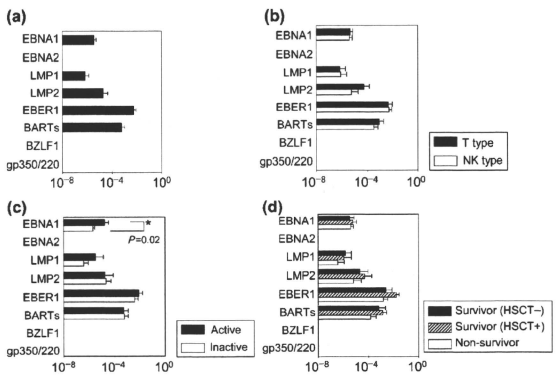

Fig. 4. EBV gene expression profile for patients with CAEBV. The quantity of each EBV gene was analysed by real-time RT-PCR and compared with the β2 m level; the mean ± SE (boxes and bars) was calculated for each gene. (a) Average expression of EBV genes in 24 patients with CAEBV. (b) Comparison between T- (13 cases) and NK- (11 cases) cell-types. (c) Comparison between clinically active (8 cases) and inactive (16 cases) patients. (d) Comparisons of surviving patients without HSCT (6 cases), surviving patients with HSCT (10 cases) and non-surviving patients (8 cases). The Mann–Whitney *U*-test was used to compare the expression values between the groups, while the analysis of variance was used to compare the groups of three.

Finally, to eliminate any potential influence of therapeutic interventions, we excluded six patients who had received therapy before entering our hospital and re-evaluated the expression of each gene in the remaining 18 patients. The level of EBNA1 expression in the active patients was 8.2 times higher than that in the inactive patients ($P=0.03$) and the rate of EBNA1-positive patients was significantly higher in the active group (83 versus 25 %; $P=0.04$). We also re-evaluated the disease outcome in these 18 patients. No significant difference was observed in the gene expression profiles between the three groups according to outcome (data not shown).

DISCUSSION

Analysing the expression profile of EBV-related genes is essential to clarify the pathogenesis of EBV-associated diseases and to uncover information regarding the prognosis of individual patients and potential therapeutic interventions. In recent years, a quantitative method for the analysis of EBV gene expression has been applied to infectious mononucleosis (Weinberger *et al.*, 2004), Burkitt's lymphoma and nasopharyngeal carcinoma (Bell *et al.*, 2006). In the present study, we quantified the expression of six latent genes and two lytic genes in 24 patients with CAEBV using one-step multiplex real-time RT-PCR. To our knowledge, this is the first study to quantify EBV gene expression in CAEBV patients. EBNA1, LMP1, LMP2, EBER1 and BARTs were detected in the patient samples, whereas EBNA2 and the two lytic genes were not detected. The gene expression pattern was latency type II, consistent with previous qualitative RT-PCR results (Kimura *et al.*, 2005). Because the lytic genes BZLF1 and gp350/220 were undetected, a lytic infection is unlikely in the peripheral blood of the CAEBV patients. EBER1 and BARTs were detected in abundance in all patients, while LMP2 was found in most patients. EBNA1 and LMP1 were less frequently detected and had lower expression levels than EBER1 and BARTs. These results are in contrast with similar analyses using T or NK cell lines, in which EBNA1, LMP1, LMP2, EBER1 and BARTs were abundantly and comparably expressed. EBNA1, EBNA2 and EBNA3C are the dominant targets of $CD4^+$ T-cell responses, while EBNA3A, EBNA3B and EBNA3C are the dominant targets of $CD8^+$ T-cell responses (Hislop *et al.*, 2007). In those patients with CAEBV, most or all of these antigens were not expressed, contributing to the evasion of cellular immunity. The decreased frequency and low expression level of EBNA1 may also contribute to the immunological escape mechanism of CAEBV.

The expression profile identified in this study may be useful for obtaining information regarding potential immunotherapies. The EBV-related antigens expressed by infected cells are possible targets for treatment with EBV-specific CTLs. Several studies have reported the use of such therapies for CAEBV, but most have shown only limited effectiveness (Hagihara *et al.*, 2003; Kuzushima *et al.*, 1996; Savoldo *et al.*, 2002). These studies used EBV-specific CTLs that were generated from LCL and targeted latency type III antigens. Our results indicate that EBER1 and BARTs were the most frequently and abundantly expressed EBV genes, followed by LMP2. Because very little EBER1 and BARTs mRNA is translated into protein (Arrand & Rymo, 1982; Kieff & Rickinson, 2007), LMP2 would be the most favourable target for CTL therapy against CAEBV. Recently, EBV-specific CTLs targeted against LMP2 were used to treat Hodgkin's lymphoma and nasopharyngeal carcinoma, both of which are latency type II infections (Bollard *et al.*, 2004, 2007; Straathof *et al.*, 2005). Furthermore, patients with CAEBV generally lack LMP2-specific CTLs (Sugaya *et al.*, 2004). However, to develop effective and useful forms of immunotherapy, additional studies focusing on the nature of the infected cells and the underlying pathology of CAEBV are necessary.

In this study, we quantified the relative expression of EBV latent and lytic genes by real-time RT-PCR. There are a few drawbacks to our system. Firstly, we used β2-microglobulin (β2 m) as a reference for relative quantification; however, comparisons of the levels of expression between different genes may be compromised by variations in the efficiency of the primers used. Another option for such quantification is preparing a standard curve for each cDNA by diluting the plasmid and estimating the number of RNA copies to quantify the expression of each gene more accurately. Secondly, we determined the type of latency based on the patterns of viral gene expression. Promoter usage for EBNA1 is different between latency types I/II and III (Qp versus Cp) (Kieff & Rickinson, 2007). Primers capable of distinguishing between the two EBNA1 promoters would enable us to confirm the type of latency more accurately. Bell *et al.* (2006) used such a system to distinguish latency types and quantify gene expression using different EBNA1 primers.

There are several possible reasons why EBNA1 and LMP1 were detected less frequently in our analysis. First, EBV-infected T or NK cells in some patients with CAEBV may indeed express very little LMP1 or EBNA1. A previous experiment performed using nested RT-PCR, which is sensitive but not quantitative, showed that these genes were expressed in less than half of CAEBV patients (Kimura *et al.*, 2005). Second, the sensitivity of the test may be too low to detect these genes. However, those samples with a low EBV DNA load in this study were not always negative for EBNA1 or LMP1, indicating that low sensitivity was not the only reason that the expression of these genes was not detected. Moreover, EBV polymorphisms may have affected our results. Indeed, the primers used for LMP1 are specific for polymorphic regions (Kubota *et al.*, 2008). However, we used mixed primers for LMP1 to account for sequence variations, and the EBNA1 primers were designed to recognize fairly conserved regions. Furthermore, we also examined EBNA1- or LMP1-negative samples by nested RT-PCR using alternate primer sets (Kimura *et al.*, 2005).

Neither EBNA1 nor LMP1 was detected in any of the samples by nested PCR (data not shown).

EBNA1 was detected more frequently and abundantly in the clinically active patients. EBNA1 is the only EBV protein consistently expressed in all proliferating cells, and it plays central roles in the maintenance and replication of the episomal EBV genome. EBNA1 also has a role in cell growth and survival (Kieff & Rickinson, 2007; Thorley-Lawson & Gross, 2004). Recently, Saridakis *et al.* (2005) demonstrated that EBNA1 inhibits apoptosis by binding to USP7, which destabilizes p53. Together with our results, these findings suggest that EBNA1 plays an important part in the pathogenesis and symptoms of CAEBV.

EBV gene expression has been shown to be related to the prognosis of EBV-associated diseases. Kwon *et al.* (2006) evaluated EBER and LMP1 expression in patients with Hodgkin's lymphoma, while Tsang *et al.* (2003) reported a relationship between the recurrence and detection of LMP1 in patients with nasopharyngeal carcinoma. Similarly, we evaluated the relationship between EBV gene expression and the prognosis of CAEBV, but were unable to identify a significant link. Other factors that may have influenced the results of this study include the small sample size, short observation period and therapeutic interventions such as HSCT. Additional studies with a greater number of cases and a longer observation period are necessary to reach conclusions about the prognostic value of EBV gene quantification for CAEBV. In conclusion, we applied a real-time RT-PCR system to PBMCs from patients with CAEBV and identified the expression profiles of several EBV genes. Quantifying EBV gene expression may be useful in clarifying CAEBV pathogenesis and provide further information about therapeutic interventions, such as CTL therapy.

METHODS

Cell lines. The EBV-positive B cell lines used in this study were Raji, Akata, lymphoblastoid cell line (LCL)-1 and LCL-2. BJAB, an EBV-negative B cell line, was used as a negative control. The EBV-positive T cell lines used were SNT-8, -13, -15 and -16 (Zhang *et al.*, 2003). The EBV-positive NK cell lines used were SNK-1, -6 and -10 (Zhang *et al.*, 2003) and KAI-3 (Tsuge *et al.*, 1999). The T/NK cell lines were derived from patients with CAEBV or nasal NK-/T-cell lymphomas.

Patients. Twenty-four patients (13 males and 11 females) with CAEBV, ranging in age from 3 to 26 years (median age 13 years), were enrolled in this study (Table 1). Each patient met the following diagnostic criteria: EBV-related symptoms for at least 6 months (e.g. fever, persistent hepatitis, extensive lymphadenopathy, hepatosplenomegaly, pancytopenia, uveitis, interstitial pneumonia, hydroa vacciniforme or hypersensitivity to mosquito bites), an increased EBV load in either the affected tissue or peripheral blood, and no evidence of previous immunological abnormalities or other recent infections that could explain the condition (Kimura, 2006; Kimura *et al.*, 2001). Based on the infected cell type, 13 patients were identified as having T-cell-type CAEBV, while 11 were identified as having NK-cell-type CAEBV. To determine which cells harboured the most EBV, peripheral blood mononuclear cells (PBMCs) were fractionated into $CD3^+$, $CD19^+$ and $CD56^+$ cells and analysed by either quantitative PCR or *in situ* hybridization, using EBER1 as a probe, as described previously (Kimura *et al.*, 2001, 2005). The patients were defined as having a T-cell-type infection if their $CD3^+$ cells contained larger amounts of EBV DNA than their PBMCs, or if their $CD3^+$ cells gave a positive hybridization signal with EBER1. The patients were defined as having an NK-cell-type infection if their $CD56^+$ cells, rather than their $CD3^+$ cells, were the major cells harbouring EBV. The EBV DNA copy numbers in each cell population are shown in Table 1.

Peripheral blood was collected at the time of diagnosis or referral to our hospital. Six of 24 patients had already received steroid therapy or chemotherapy. PBMCs were isolated using Ficoll–Paque density gradients (Pharmacia Biotech) and stored at −80 °C until further use. Eight patients with severe symptoms such as high fever, distinct hepatosplenomegaly, and/or elevated hepatic transaminase levels at the time of sample collection were defined as having clinically active disease, while 16 patients with no symptoms or with only skin symptoms, including hydroa vacciniforme, were defined as having inactive disease. Eight of the patients died after 1–49 months of observation (median 14 months). Sixteen of the patients, 10 of whom received HSCT, were alive after 9–115 months of observation (median 28 months). Twenty-three healthy carrier volunteers who were seropositive for EBV and three patients with infectious mononucleosis (aged 5, 11 and 29 years) were enrolled as controls.

Informed consent was obtained from all patients or their guardians. The institutional review board of Nagoya University Hospital approved the use of the specimens that were examined in this study.

Real-time PCR assay. DNA was extracted from 1×10^6 PBMCs using a QIAmp blood mini kit (Qiagen). EBV DNA was quantified by real-time PCR as described previously. The viral load is expressed as the number of copies $(\mu g\ DNA)^{-1}$ (Kimura *et al.*, 1999).

RNA was extracted from 1×10^6 cells using a QIAmp RNeasy mini kit (Qiagen). Contaminating DNA was removed by on-column DNase digestion using the RNase-free DNase set (Qiagen) (Kubota *et al.*, 2008). Viral mRNA expression was quantified by one-step multiplex real-time RT-PCR using an Mx3000P real-time PCR system (Stratagene) as described previously (Kubota *et al.*, 2008). All of the primer/probe combinations, except those for EBER1 lacking an intron, were designed to span introns to avoid amplifying residual genomic DNA. The primer and probe sequences are listed in Supplementary Table S1 (available in JGV Online). The primers used for EBNA1, EBNA2, LMP1 and BZLF1, which were described previously (Kubota *et al.*, 2008), were modified according to sequence variations amongst the strains. The stably expressed housekeeping gene $\beta 2$ m was used as an endogenous control and reference gene for relative quantification (Patel *et al.*, 2004).

Cell sorting and gene expression analysis. $CD3^+$, $CD19^+$ and $CD56^+$ cells were separated from 1×10^7 PBMCs by immunomagnetic sorting using anti-CD3, -CD19 and -CD56 MACS Microbeads, respectively (Miltenyi Biotec). After two rounds of sorting, the purity of the populations exceeded 95 %. RNA was extracted from each cell population for real-time RT-PCR analysis. For comparison, RNA was also extracted from unsorted PBMCs.

Statistical analyses. All statistical analyses were performed using StatView (version 5.0; SAS Institute). Geometric (logarithmic) means were calculated for the expression of each EBV gene. For the negative samples, the default value, which was defined as the lowest level of expression for a particular gene, was used for the calculation. The default values for the undetected genes EBNA1, LMP1 and LMP2 were 10^{-6}, 10^{-8} and 10^{-8}, respectively. The Mann–Whitney *U*-test was used to compare the expression levels between groups, while analysis of variance was used to compare three groups. Fisher's exact